Journal of Biochemistry and Molecular Biology, Vol. 35, No. 2, March 2002, pp. 143-154

JOURNAL OF Biochemistry and Molecular Biology

Acid and Chemical Induced Conformational Changes of Ervatamin B. Presence of Partially Structured Multiple Intermediates

Monica Sundd[1], Suman Kundu[2] and Medicherla V. Jagannadham*
Molecular Biology Unit, Institute of Medical Sciences, Banaras Hindu University, Varanasi-221005, India

Received 11 June 2001, Accepted 21 September 2001

The structural and functional aspects of ervatamin B were studied in solution. Ervatamin B belongs to the α + β class of proteins. The intrinsic fluorescence emission maximum of the enzyme was at 350 nm under neutral conditions, and at 355 nm under denaturing conditions. Between pH 1.0-2.5 the enzyme exists in a partially unfolded state with minimum or no tertiary structure, and no proteolytic activity. At still lower pH, the enzyme regains substantial secondary structure, which is predominantly a β-sheet conformation and shows a strong binding to 8-anilino-1-napthalene-sulfonic acid (ANS). In the presence of salt, the enzyme attains a similar state directly from the native state. Under neutral conditions, the enzyme was stable in urea, while the guanidine hydrochloride (GuHCl) induced equilibrium unfolding was cooperative. The GuHCl induced unfolding transition curves at pH 3.0 and 4.0 were non-coincidental, indicating the presence of intermediates in the unfolding pathway. This was substantiated by strong ANS binding that was observed at low concentrations of GuHCl at both pH 3.0 and 4.0. The urea induced transition curves at pH 3.0 were, however, coincidental, but non-cooperative. This indicates that the different structural units of the enzyme unfold in steps through intermediates. This observation is further supported by two emission maxima in ANS binding assay during urea denaturation. Hence, denaturant induced equilibrium unfolding pathway of ervatamin B, which differs from the acid induced unfolding pathway, is not a simple two-state transition but involves intermediates which probably accumulate at different stages of protein folding and hence adds a new dimension to the unfolding pathway of plant proteases of the papain superfamily.

Keywords: Plant cysteine proteases, Ervatamin B, Protein folding, Cooperative transitions, Intermediate

*To whom correspondence should be addressed.
Tel: 91-542-367936; Fax: 91-542-367568
E-mail: jvm@banaras.ernet.in

Present Address
[1]Department of Biochemistry, University of Iowa, Iowa City, IA 52242, USA
[2]Department of Biochemistry, Biophysics and Molecular Biology, Iowa State University, Ames, IA 50011, USA

Introduction

An interplay of various physicochemical forces - like hydrophobic interactions, ionic interactions, disulfide bonds, and other local as well as non-local interactions - maintain the three-dimensional structure of proteins. The conformational stability of the native protein is a function of external variables, such as temperature, pH, ionic strength, and solvent composition. A quantitative analysis of the role of these variables in the structure formation is a requisite for the description of the forces that are responsible for the conformational stability, which in turn can provide insight into the molecular structure of the enzyme. A simple method for such studies involves the monitoring of conformational changes that are caused upon perturbation of a protein molecule by various agents, such as acid, GuHCl, or urea.

With this view, conformational studies in solution have been initiated with ervatamin B, a novel plant cysteine protease that was isolated in our laboratory from the latex of a medicinal plant *Ervatamia coronaria* (Kundu *et al.*, 2000). Ervatamin B seems to be a potential endopeptidase with many interesting features and probable applications. Ervatamin B (approximate M_r 26, 000) has been biochemically characterized, and the preliminary X-ray analysis has been reported (Chakrabarti *et al.*, 1999). Ervatamin B probably shares an ancestral gene with papain (21 N-terminal amino acid residues showed a 57% sequence identity to papain). In many ways ervatamin B is distinct from papain, ervatamin C, and other cysteine proteases in terms of half cysteines (five) content, stability, etc., therefore, it is worth studying. The present investigation describes the biophysical characterization of ervatamin B in an endeavor to understand the structure-function relationship, the basis, and rationale of its physicochemical properties, as well as its

folding-unfolding mechanism.

The folding mechanism of many small globular proteins is described in terms of the two-state model (Privalov, 1979), where either native or denatured states are highly populated. However, it has been shown that such phenomenon occurs through some kinetic intermediates that accumulated during the folding process (Ptitsyn, 1995; Gast *et al*., 1998). Protein folding involves a discrete pathway with the formation of intermediate states between the native and denatured states (Kim and Baldwin, 1990). It is also argued that the equilibrium molten globule state, which is observable under artificial conditions, such as low pH and low denaturant concentrations, may also be involved in physiological processes in the living cell (Bychkova *et al.*, 1996). Therefore, the identification and characterization of the intermediate states that are populated during the folding process has received considerable attention, and a lot of effort is being made in this direction. These efforts yielded common characteristics to the intermediate states, especially that compact collapsed states with significant secondary structure appear in the folding process for a number of proteins (Khorasanizadeh *et al.*, 1993; Kuwajima *et al.*, 1993). The species (observed at equilibrium for a large number of proteins under mild denaturing conditions with properties of partially-folded states) made possible the study in real-time scale experiments. Such intermediates from different proteins of different structure types have some common characteristics, and are termed as "molten globule" to emphasize the possible occurrence of such an intermediate as a general physical state of globular proteins (Ptitsyn *et al.*, 1990; Harding *et al.*, 1991; Arai and Kuwajima, 1996).

There is not much information available about the molten globule state in multidomain proteins and its role in protein folding. It has been proposed that domains in the native molecules are independent folding units that assemble and produce native molecules (Garel, 1992). These structural regions are expected to fold independently, whether they are isolated or together. However, further studies in this respect are necessary. Studies on the different conformational states in the unfolding-refolding of multidomain proteins are important for an understanding of the principles that govern protein folding (Dobson, 1992).

The paradigm enzyme papain and other plant cysteine proteases that belong to the papain superfamily usually consist of two well-defined domains; therefore, they provide an excellent system for studies in understanding the folding-unfolding behavior of proteins in general and multidomain proteins in particular. Very little information is available about the general folding aspects of plant cysteine proteases of the papain family. All investigations so far have mainly involved papain (Hernandez-Arana and Soriano-Garcia, 1988; Xiao *et al.*, 1993). Detailed studies regarding the intermediates and their role in the folding of papain have been recently initiated in our laboratory (Edwin and Jagannadham, 1998). Another novel cysteine protease ervatamin C, with remarkable stability, was also isolated in our laboratory (Sundd *et al.*, 1998). It has also been used as a model system to elucidate the folding behavior of plant cysteine proteases in particular (Kundu *et al.*, 1999). Thus, studies about the individual variations within a family would certainly help to generalize the folding behavior of enzymes of the papain superfamily, and would complement their proposed mechanisms.

Materials and Methods

Materials Fresh latex, obtained from young stems of the plant *Ervatamia coronaria*, was used to purify the enzyme ervatamin B, as described previously (Kundu *et al.*, 2000). Sodium tetrathionate was used throughout the purification procedure to avoid any complications due to autodigestion, and this inactive enzyme was used for all of the biophysical studies reported here. All of the physical properties of the enzyme are the same in both the active and inactive forms. Concentration of the enzyme was determined by spectrophotometry using an extinction coefficient $\varepsilon^{1\%}_{1cm}$ = 20.5 at 280 nm (Kundu *et al*., 2000) and also by Bradford assay. All other materials were as described previously (Kundu *et al.*, 1999).

Absorbance spectroscopy Absorbance measurements were carried out on a Beckman DU-640B spectrophotometer that was equipped with a constant temperature cell holder. Protein concentration for all absorbance measurements was between 6 and 10 μM. Absorbance spectra were recorded between 260 and 320 nm.

Fluorescence spectroscopy Fluorescence measurements were carried out on a Perkin-Elmer LS-5B spectrofluorometer that was equipped with a constant temperature cell holder. Protein concentration was between 0.015-0.025 mg/ml. For tryptophan fluorescence of ervatamin B, the excitation was at 292 nm and emission was recorded from 300 to 400 nm with 10 and 5 nm slit widths for excitation and emission, respectively. For ANS fluorescence, the excitation was at 380 nm. The emission spectra were collected between 400 and 600 nm with the same slit widths for excitation and emission as above.

Spectropolarimetric studies CD measurements were done on a JASCO J-500A spectropolarimeter that was equipped with a 500 N data processor. Conformational changes in the secondary structure were monitored in the region between 200 and 260 nm with a protein concentration of 0.1 mg/ml in a cuvette of 1 mm pathlength. Changes in the tertiary structure were observed in a 10 mm path length cuvette in the region between 260 and 320 nm at a protein concentration of 0.7 mg/ml. After subtracting appropriate blanks, mean residue ellipticities were calculated, using the formula (Balasubramanian and Kumar, 1976) $[\theta] = \theta_{obs} \times MRW/10cl$, where θ_{obs} is the observed ellipticity in degrees, MRW is the mean residue weight, c is the concentration of protein in g/ml, and l is the path length in cm. A mean residue molecular weight 110 was used. A sensitivity of 1 m°/cm was used for far-UV measurements, and 2 m°/cm was used for near-UV measurements.

Acid denaturation of ervatamin B in presence and absence of salt Acid denaturation of ervatamin B was carried out as a function of pH using the following: KCl-HCl (pH 0.5-1.5), Gly-HCl (pH 2.0-3.5), sodium acetate (pH 4.0-5.5), sodium phosphate (pH 6.0-8.0), Tris-HCl (pH 8.5-10.5), and Gly-NaOH (pH 11.0-12.5). Concentrations of all of the buffers were 50 mM. A stock solution of the protein was added to the appropriate buffer, and incubated for 24 h at 25°C. The final pH and concentration of the samples were measured again. Acid denaturation was also performed at various pH in the presence of increasing concentrations of KCl.

Guanidine hydrochloride and urea induced unfolding Chemically induced denaturation of the enzyme at a given pH was performed at different concentrations of denaturants. Protein samples were incubated at the desired denaturant concentration for approximately 24 h at 25°C to attain equilibrium. The final concentration of the protein and denaturant were measured by spectrophotometry and refractive index, respectively. All of the unfolding transitions are analyzed as described (Shirley, 1995) in order to obtain transition midpoints, as well as to judge the cooperativity or non-cooperativity of the transitions. To obtain the transition midpoints from an equilibrium solvent denaturation curve, the regions of the curve preceding and following the transitions were fit to a straight line. For a comparison of the results that were obtained by various measures (molar ellipticity, fluorescence intensity, emission maximum, and relative activity), they were normalized and expressed as a fraction of the native protein that was unfolded (fraction unfolded). There f_u was calculated as $f_u = (X_n - X_{obs}) / (X_n - X_u)$, where X_n is the signal for the native protein, X_u is the respective signal of the denatured protein, and X_{obs} is the observed signal under given conditions. X_n and X_u were obtained by extrapolation of the linear dependency of the signal on the concentration of the denaturant in the regions before and after transition, respectively. All of the spectroscopic measurements (at different concentrations of the denaturant) were performed against appropriate blanks that contained the denaturant in the absence of the enzyme.

Assay for enzyme activity The hydrolyzing activity of the enzyme (under various conditions of pH and in the presence of chemical denaturant) was monitored using the denatured natural substrate azoalbumin, following the described procedure (Kundu *et al.*, 2000). A control assay was performed with no enzyme in the reaction mixture and used as a reference. To monitor the effects of pH on the enzyme activity, the enzyme was equilibrated in a buffer of the prescribed pH for 24 h. The aliquots were assayed separately, both at the same pH and at neutral pH. The enzyme assays could not be done below pH 4.0 since azoalbumin is insoluble. Therefore, the enzyme activity was checked below pH 4.0 using denatured hemoglobin as a substrate. In the case of denaturants, the enzyme was incubated overnight at the prescribed concentrations of the denaturant solution. The remaining activity was measured as previously described. The activity of the enzyme in the absence of denaturant was used as a reference.

ANS Binding Assay Exposure of hydrophobic surfaces in the enzyme was measured by its ability to bind to the fluorescent dye ANS (Semisotnov *et al.*, 1991). A stock solution of ANS was prepared in methanol. The concentration of ANS was determined using an extinction coefficient of $\varepsilon = 5000\ M^{-1}\ cm^{-1}$ at 350 nm (Khurana and Udgaonkar, 1994). The protein was incubated with a 100-fold molar excess of ANS for more than 30 min in darkness at room temperature, and ANS fluorescence was measured. The protein concentration was 0.015-0.05 mg/ml.

Results

CD spectra The CD spectra of native and denatured ervatamin B at pH 7.0 are shown in Fig. 1.

In the aromatic region, the CD spectrum of native ervatamin B exhibits a positive peak that is centered at 278 nm (Fig. 1A), and a negative band that is centered at 295 nm. At the latter wavelength, tyrosine and phenylalanine residues do not contribute to the CD spectra of proteins (Strickland *et al.*, 1969; Strickland, 1974), and the negative band probably

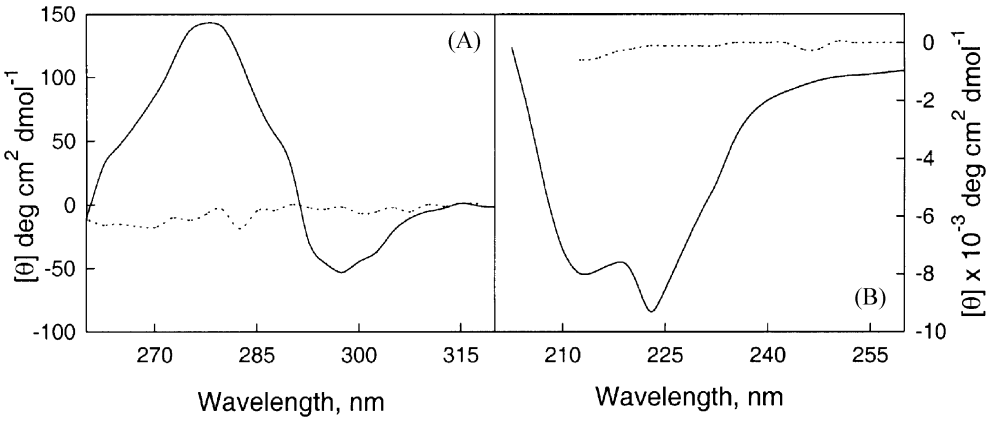

Fig. 1. CD spectra of native and denatured ervatamin B. (A) Near and (B) far-UV CD spectra of ervatamin B at (–) pH 7.0 and (---) 6M GuHCl. The samples were incubated for 24 h at 25°C before the measurements. Protein concentration was 0.1mg/ml for far-UV CD and 0.7 mg/ml for near-UV CD.

originates from tryptophan residues that are located in an asymmetrical environment (Solis-Mendiola, 1992). The intensity of the negative band at 297 nm is also much lower than the positive peak at 276-278 nm.

In the far-UV region, native ervatamin B revealed two well-resolved negative peaks at 222 nm and 208 nm (Fig. 1B). The signal at 222 nm was greater in magnitude, which indicates the enzymes high level of structural integrity. The shape of the spectra, and strong negative ellipticities at 208, 215 and 222 nm, suggest that ervatamin B is composed of α-helix and β-sheet rich regions. It also appears to belong to the α + β class of proteins (Manavalan and Johnson, 1983). The mean residue ellipticity at 222 nm was $-9.1 \pm 0.5 \times 10^3$ deg.cm^2 dmol^{-1}. It can be used to determine the α-helicity of the protein by using the following simple calculation (Chen *et al.*, 1972): %α-helicity = $(\theta_{222} - \theta_{min} / \theta_{max} - \theta_{min}) \times 100$, where $\theta_{222\ nm}$ is the molar ellipticity of the observed protein, $\theta_{min} = 2340$ is the minimum value of the molar ellipticity at 222 nm that was calculated for the "unordered" fraction of five proteins, and $\theta_{max} = 30{,}300$ is the maximum value for the ellipticity at 222 nm, as measured for the helical fraction of the five proteins. The estimated α-helicity of ervatamin B is approximately 22% at neutral pH.

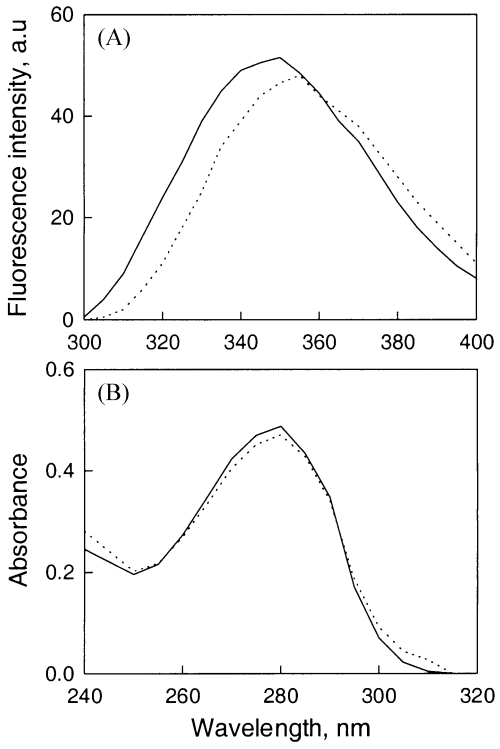

Fig. 2. Fluorescence and absorbance spectra of ervatamin B. (A) Intrinsic fluorescence spectra of ervatamin B at (–) pH 7.0 and in (---) 6 M GuHCl. Protein concentration was 0.025 mg/ml. The excitation wavelength was 292 nm with slit widths of 10 nm and 5 nm for excitation and emission, respectively. (B) Absorbance spectra of ervatamin B at (–) pH 7.0 and in (---) 6 M GuHCl. The samples were incubated for 24 h at 25°C before the measurements. Protein concentration was 0.16 mg/ml.

In 6M GuHCl ervatamin B loses all of its tertiary and secondary structural features. There is a complete disappearance of all of the prominent peaks in the peptide bond and aromatic regions (Fig. 1). Also, the protein is in the unfolded state (D-state).

Fluorescence spectra Fluorescence spectroscopy can provide information about the polarity of the tryptophan environment, as well as the solvent accessibility of the chromophores that are sensitive to local conformational changes at the tertiary level of folding (Schmid, 1989). Intrinsic fluorescence spectra of ervatamin B in native and completely unfolded states are shown in Fig. 2A. When excited at 292 nm, ervatamin B showed an emission maximum at 350 nm in the native state. Spectra of the unfolded enzyme in 6 M GuHCl remains similar in shape, but the emission maximum shifts from 350 nm to 355 nm with a decrease in the intensity by about 8%. This indicates that the tryptophan residues of ervatamin B are in a more polar environment than the native state, which is characteristic of unfolding.

Absorbance spectra The absorbance spectrum of the native enzyme is shown in Fig. 2B. Absorbance spectra of ervatamin B in the native and unfolded conditions show no significant differences in shape or absorbance maximum, which is at 279 nm.

Acid induced conformational changes in ervatamin B Changes in the tertiary structure of ervatamin B as a function of pH are shown in Fig. 3A. The change in ellipticity at 278 nm against pH follows a bell-shaped curve with loss of tertiary structure only beyond pH 3.0 and 11.0. The overall near-UV CD spectral characteristics remain the same between pH 3.0 and 11.0, and are typical of the native state with a positive peak at 278 nm and a negative band at 295 nm. However, the negative peak was more intense above pH 9.0; the positive peak was slightly less intense at pH 3.0. At pH 2.0 and below, all of the prominent peaks were absent, and the spectrum was identical to that in 6 M GuHCl (inset of Fig. 3A). This indicates that the enzyme lost its tertiary structure and is completely unfolded. The changes in the proteolytic activity with pH also follow a shape that is similar to the ellipticity at 278 nm (Fig. 3B). The enzyme is also fully active over the pH range 3.0-11.0 and drops only on either side of this range.

The effect of varying pH, in presence and absence of salt, on the secondary structure of ervatamin B is shown in Fig. 3C. The enzyme retained most of its secondary structure up to pH 3.0, and a gradual decrease in ellipticity values below this pH was observed. Acid induced the unfolding of the enzyme, in the absence of any salt, followed by ellipticity at 220 nm that is non-cooperative with two transitions (Fig. 3C, open circles), which indicates the presence of intermediates in the process. The first transition, from the native state to the acid unfolded

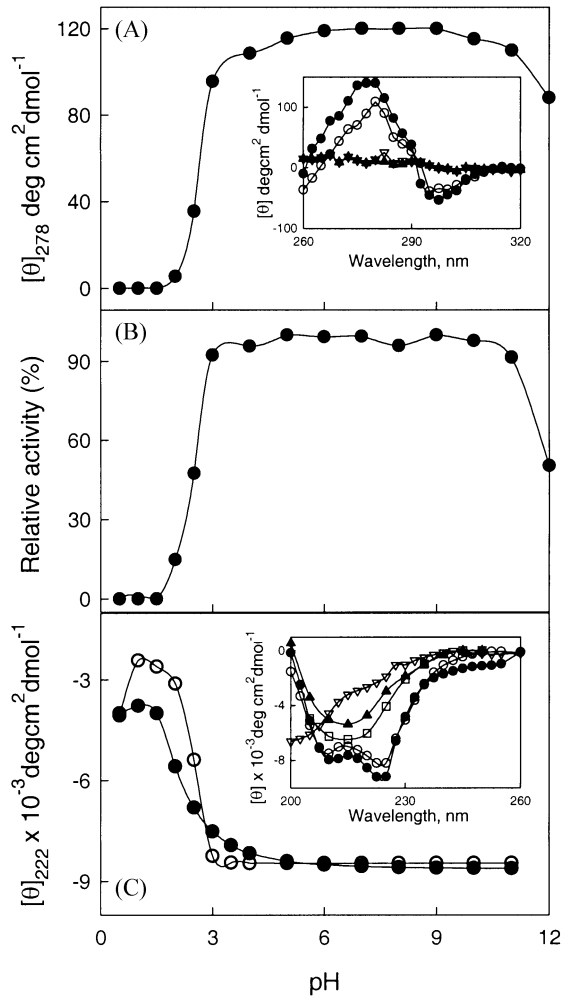

Fig. 3. pH dependent conformational changes of ervatamin B. (A) Ellipticity at 278 nm. Inset. Near-UV CD spectra at (●) pH 7.0, (○) pH 3.0, (▽) pH 2.0 and (▼) pH 0.5. Protein concentration was 0.7 mg/ml. (B) Proteolytic activity measurements at pH 7.0 were performed as described in Methods. (C) Ellipticity at 222 nm in the presence (λ) and absence (○) of 0.5 M KCl. Inset. Far-UV CD spectra at pH 7.0 (●), pH 3.0 (○), pH 2.0 (▽), pH 0.5 (▲), and 0.5 M KCl, pH 2.0 (□). Protein concentration was 0.1 mg/ml. The samples were incubated for 24 h at 25°C before the measurements.

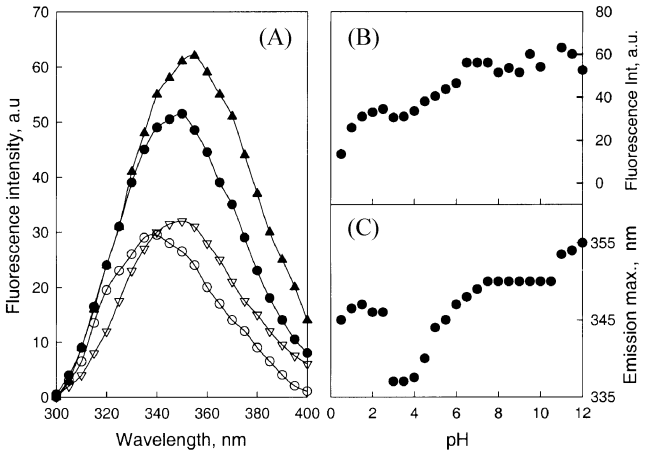

Fig. 4. Effect of pH on the intrinsic fluorescence of ervatamin B. (A) Intrinsic fluorescence spectra at (●) pH 7.0, (○) pH 3.0, (▽) pH 2.0, and (▲) pH 11.0. The changes in the (B) fluorescence intensity and (C) wavelength maxima of Trp emission. Protein concentration was 0.025 mg/ml. The excitation wavelength was at 292 nm with slit widths of 10 nm and 5 nm for excitation and emission, respectively.

state, occurs in the vicinity of pH 4.0-1.0. A similar transition is also observed in the aromatic CD region (Fig. 3A), between pH 4.0 and 1.0. It reflects the loss of the native-like tertiary structure, which is not regained at lower pH values. The spectra are similar to that of the unfolded protein in 6 M GuHCl. Such a loss of secondary, as well as tertiary structure, yields the acid-unfolded state (Fink *et al.*, 1994). This indicates incomplete unfolding that is evidenced by the residual molar ellipticity in the far-UV region compared to that in 6M GuHCl. Further addition of acid leads to a second transition between pH 1.5 and 0.5 that is manifested as an increase in secondary structure (refolding), leading to the A-state. However, the presence of 0.5 M KCl induced a cooperative transition (Fig. 3C, filled circle) between pH 4.0-0.5, with no detectable intermediates as the enzyme passes from the native state directly to the A-state, regaining a slightly higher amount of secondary structure than at pH 0.5. However, aggregation or salting out was observed at higher concentrations of added salt (> 0.5 M KCl) at pH 1.0-2.5. The far-UV CD spectra of ervatamin B at various pH are shown in the inset of Fig. 3C. Up to pH 3.0, all of the spectral features remain unchanged relative to the native state while both the negative peaks at 220-222 nm and 208 nm are lost between pH 2.5-1.0 with a marked decrease in ellipticity. However, the spectrum at pH 0.5 shows a substantial secondary structure with a negative peak at 215 nm and a positive peak at 195 nm, which is characteristic of predominant β-sheet, thus differing from either the native state or the acid unfolded state. The spectra between pH 2.5-1.0 in the presence of KCl are also similar in shape but with higher ellipticity. Hence, the addition of acid beyond pH 1.0 leads to the formation of the A-state that is characterized by the presence of significant non-native secondary structure, and the absence of tertiary structure. In the A-state (pH 0.5), the mean residue ellipticity at 215 nm and 222 nm were $-5.4 \pm 0.25 \times 10^3$ deg.cm^2 dmol^{-1} and $-4.1 \pm 0.25 \times 10^3$ deg.cm^2 dmol^{-1}, respectively. The ellipticity at 222 nm in the presence of 0.5 M KCl at pH 2.0 is $-6.4 \pm 0.5 \times 10^3$ deg.cm^2 dmol^{-1}. The change in overall ellipticity below pH 3.0 may be due to the partial unfolding of the molecule, especially the alpha helix-rich regions.

An important point is that if the protein is incubated at a given pH and the activity is measured at the same pH, then the activity is less than the value obtained when assayed under neutral conditions. However, the same sample gives an equivalent activity if assayed at neutral conditions. This

observation, combined with the fact that the secondary and tertiary structural content is intact even at low pH, shows that the enzyme is stable. It does not loose its proteolytic activity, even after a prolonged exposure to the pH range 3.0-11.0, and it is reversible to neutral pH.

The pH dependence of intrinsic fluorescence properties of ervatamin B is shown in Fig. 4. Between pH 3.0 and 11.0, where protein is stable, the emission maximum (Fig. 4C) increases from 337 nm at low pH to 353 nm at high pH with the transition midpoint at about 5.8. The fluorescence intensity (Fig. 4B) increases by a factor of two over the same pH region with a similar transition midpoint.

Typical fluorescence spectra of ervatamin B at different pH are shown in Fig. 4A. At neutral pH the wavelength emission maximum was 350 nm, and shifted to 338 nm by pH 3.0 and 4.0, while the fluorescence intensity was reduced to 53-57% of the native protein. However, there is a discontinuity in the changes of emission maximum when the protein unfolds, both in the acid region between pH 2.5 and 3.0, and in the alkaline region between pH 10.5 and 11.0. Both acid and alkaline unfolding causes an increase in emission maximum. Acid unfolding is accompanied by a further decrease in fluorescence intensity while alkaline transition is not (Fig. 4B). However, at pH 2.0 and below the emission maximum shifts again to a higher wavelength (345 nm). At and above pH 11.0, the emission maximum was at 355 nm, indicating a complete unfolding of the molecule. There, as the shift in the emission maximum upon acidification is less in magnitude, it indicates a partial unfolding. The changes in the tryptophan environment in the protein molecule on acidification have been followed by changes in the fluorescence intensity and shift in emission maximum (Fig. 4B and 4C). The pH induced transition curve, obtained by following fluorescence intensity, is non-cooperative. It shows biphasic nature with one transition between pH 0.5 to 3.5 with a midpoint of pH 1.01, and the other between pH 3.0-11.0 with a midpoint of pH approximately 5.85. The pH transition curve that was obtained by following the shift in the fluorescence emission maximum is also biphasic with a similar trend as above, but there was a drastic fall in the wavelength maximum between pH 3.0 and 4.0.

Between pH 7.0 and 3.0, the absorbance spectra are identical in shape and intensity. Below pH 3.0, however, there was only a very slight reduction in intensity without any changes in the overall shape of the spectra, hence they could not be used as an effective probe for these studies (data not shown).

GuHCl-induced unfolding The GuHCl-induced changes of ervatamin B were followed by CD (ellipticity at 278 nm and 220 nm), fluorescence (wavelength emission maximum), and activity. Under neutral conditions, the chemical-induced transition curves were sigmoidal, as seen by the different measures (Fig. 5A). All of the structural changes take place between 2.35-4.0 M GuHCl with a transition mid-point at

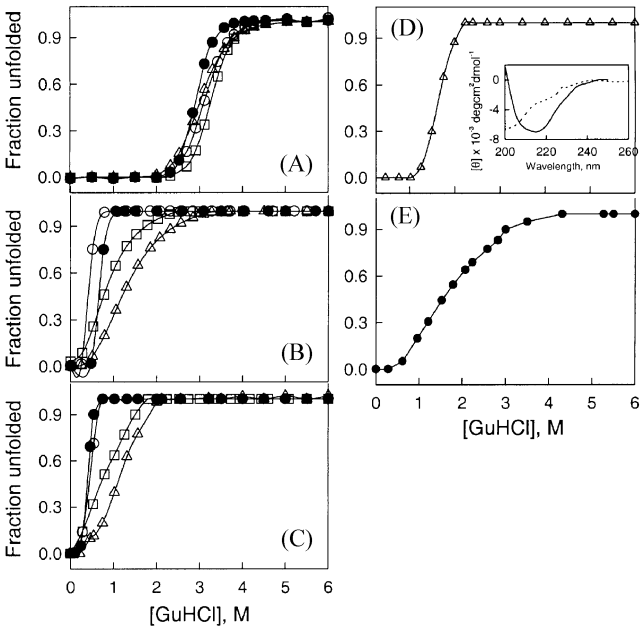

Fig. 5. Equilibrium GuHCl denaturation of ervatamin B. The unfolding of ervatamin B was monitored at (A) pH 7.0, (B) pH 4.0, (C) pH 3.0, (D) pH 2.0, and (E) pH 0.5 by change in circular dichroism ellipticity at 278 nm (●), in circular dichroism ellipticity at 222 nm (△), in proteolytic activity (○), and in wavelength of maximum emission (□) arising from excitation at 292 nm. The resulting data were normalized to fractions of unfolded protein and plotted. The samples were incubated in GuHCl for 24 h at 25°C before the measurements. Inset of (D): Far-UV spectra at pH 2.0 in presence (–) and absence (---) of 0.25 M GuHCl.

3.1 ± 0.1 M GuHCl. Upon unfolding of the molecule, no significant change in fluorescence intensity was seen, but the emission maximum suffered a shift of 5 nm. The loss in proteolytic activity coincided with the loss in tertiary and secondary structures, which reflects a good correlation between the activity and structural integrity of the molecule. Thus, ervatamin B is structurally and functionally stable up to 2.35 M GuHCl.

Since ervatamin B was structurally stable with no irreversible loss of proteolytic activity, even after a prolonged exposure to a wide range of pH (3-11), it was important to check the structural integrity of the molecule at low pH. Any subtle changes in the structure of the enzyme upon acidification should reflect its stability, and can be seen in its behavior towards denaturants.

The GuHCl-induced denaturation of ervatamin B at pH 4.0 is shown in Fig. 5B. The unfolding transition curves, measured by different methods, are sigmoidal and non-coincidental with the activity, tertiary structure, intrinsic fluorescence, and secondary structure being lost in this order. The transition midpoints (c_m) were 0.46 ± 0.1, 0.51 ± 0.1, 0.86 ± 0.1, and 1.14 ± 0.1 M GuHCl, respectively. Denaturation of ervatamin B starts at a very low concentration of GuHCl at

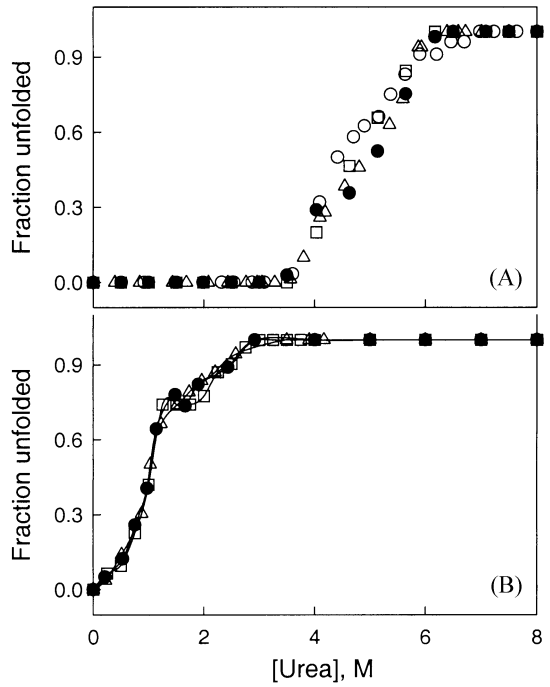

Fig. 6. Equilibrium urea denaturation of ervatamin B. (A) At pH 4.0. and (B) at pH 3.0. The unfolding of ervatamin B was monitored by a change in circular dichroism ellipticity at 278 nm (●), in circular dichroism ellipticity at 222 nm (△), in proteolytic activity (○), and in wavelength of maximum emission (□) arising from excitation at 292 nm. The resulting data were normalized to fractions of unfolded protein and plotted.

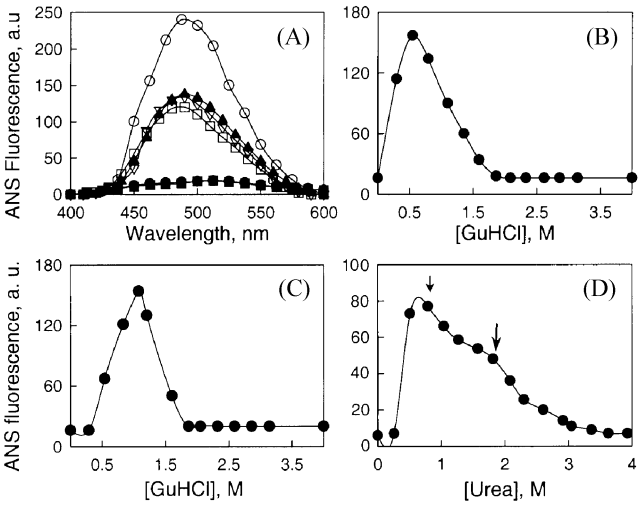

Fig. 7. Binding of ANS to ervatamin B under various conditions. (A) ANS binding to ervatamin B in (●) pH 7.0, (■) 6 M GuHCl, (○) pH 2.0, (▲) pH 0.5, (▽) pH 2.0 with 0.5 M KCl, and (□) 0.25 M GuHCl, pH 2.0. Protein concentration was 0.015 mg/ml. ANS binding during GuHCl-induced unfolding (B) at pH 3.0 and (C) at pH 4.0. The ANS fluorescence intensity at 480 nm was followed at protein concentrations of 0.015 and 0.025 mg/ml, respectively. (D) ANS binding to ervatamin B during urea denaturation at pH 3.0. Two ANS binding concentrations are indicated by arrow. Protein concentration was 0.015 mg/ml. In all of the cases, the protein was incubated in darkness with a 100-fold molar excess of ANS for more than 30 min at room temperature, and ANS fluorescence was measured with an excitation at 380 nm.

this pH (4.0). Loss in activity and tertiary structure took place between 0.25 and 1.0 M GuHCl, whereas the secondary structural changes occurred between 0.25 M and 2.5 M GuHCl. Changes in intrinsic fluorescence occurred between 0.25 M and 3.0 M GuHCl. Fluorescence intensity, however, showed no significant change (data not shown).

The overall characteristics of the GuHCl-induced unfolding of ervatamin B at pH 3.0 were similar to that observed at pH 4.0 (Fig. 5C). Also, the activity and other structural parameters were lost in the same order, but with lower mid-points of 0.42 ± 0.1, 0.46 ± 0.1, 0.79 ± 0.1, and 1.16 ± 0.1 M GuHCl for proteolytic activity, tertiary structure, intrinsic fluorescence, and secondary structure, respectively.

When pH is further lowered below 3.0, the protein looses all the tertiary structure with a complete loss of proteolytic activity. The GuHCl unfolding of ervatamin B at pH 2.0 was followed by far-UV CD (Fig. 5D). The loss in secondary structure followed a single transition with a transition midpoint at 1.64 ± 0.1 M GuHCl. Thus, GuHCl completely unfolds the partially denatured acid unfolded state of ervatamin B. It is to be noted that at a low concentration of GuHCl (0.25 M), far-UV CD spectra is predominantly β-sheeted, similar to the spectra of the protein in the A-state that is seen in acid-induced unfolding (inset of Fig. 5D). The ellipticity at 215 nm in this state is $-7.04 \pm 0.5 \times 10^3$ deg.cm^2 dmol^{-1}. GuHCl stabilizes this state and it shows a transition mid-point that is higher than those at pH 3.0 and 4.0.

Similarly, the GuHCl induced unfolding of ervatamin B at a very low pH (0.5) was also a single transition (Fig. 5E). The transition mid-point is 1.61 ± 0.1 M GuHCl, as in the case of a similar measurement at pH 2.0.

Urea induced unfolding Under neutral conditions, urea induced no structural perturbations to the protein molecule, and ervatamin B exhibits all of the proteolytic activity. However, urea-unfolding studies at as low a pH as 4.0 and 3.0 yielded some interesting results. At pH 4.0, the urea induced changes that resulted (by various measures) in a single sigmoidal transition curve (Fig. 6A) with all the changes that occur between 3.5-6.5 M urea. The transition midpoints (c_m) of the denaturation followed by different measures (activity, near-UV CD, far-UV CD and wavelength maximum), are approximately at 4.75 ± 0.15 M. Emission maximum of intrinsic fluorescence shifted by 5 nm upon urea unfolding, and the fluorescence intensity changed little (data not shown). The loss in proteolytic activity upon unfolding, within the range of error, coincides with the loss in tertiary and secondary structures. This reflects a good correlation between the activity and structural integrity of the molecule. Thus,

ervatamin B is structurally and functionally stable up to 3.5 M urea concentration at pH 4.0.

At pH 3.0, urea-induced unfolding of ervatamin B takes place at very low concentrations of the denaturant, and the unfolding characteristics are different from those observed at pH 4.0. All of the structural and functional changes occur between 0.25 and 3 M urea, and the transition curves are coincidental. Further, the individual transitions that were observed by various measures are biphasic in nature (Fig. 6B). Initially, the structure and function of ervatamin B disappeared rapidly up to 1.5 M urea with no further significant changes up to 1.75 M urea, and followed by a slow decrease beyond this concentration. The c_m in the region of rapid fall is at 0.937 ± 0.1 M urea, while the latter is at 2.16 ± 0.1 M urea. However, at pH 2.0, low concentrations of urea induced no structure in the enzyme, as in the case of GuHCl.

ANS binding ANS preferentially binds to the enzyme in the A-state (pH 0.5 or pH 0.5-2.5 in presence of 0.5 M KCl or in 0.25 M GuHCl at pH 2.0), compared to the native and completely unfolded states (Fig. 7A). ANS fluorescence intensity increases approximately five-fold, and the emission maximum shifts to a shorter wavelength (490 nm), when compared to the native or denatured states (515 nm). However, the extent of ANS binding to ervatamin B at pH 2.0, in the presence of salt (0.5 M KCl), or a low denaturant (0.25 M GuHCl), is less than the binding that is seen in the absence of salt or a denaturant.

The extent of ANS binding to ervatamin B was also followed throughout the GuHCl and urea denaturation. Strong ANS binding to the protein was observed at low concentrations of GuHCl, both at pH 3.0 (Fig. 7B) and 4.0 (Fig. 7C). ANS fluorescence intensity increased approximately eight-fold, and the emission maximum shifted to a shorter wavelength (480 nm) compared to the native state (515 nm). The ANS binding was at the maximum during GuHCl unfolding at 0.5 ± 0.1 M GuHCl and 1.1 ± 0.1 GuHCl at pH 3.0 and 4.0, respectively.

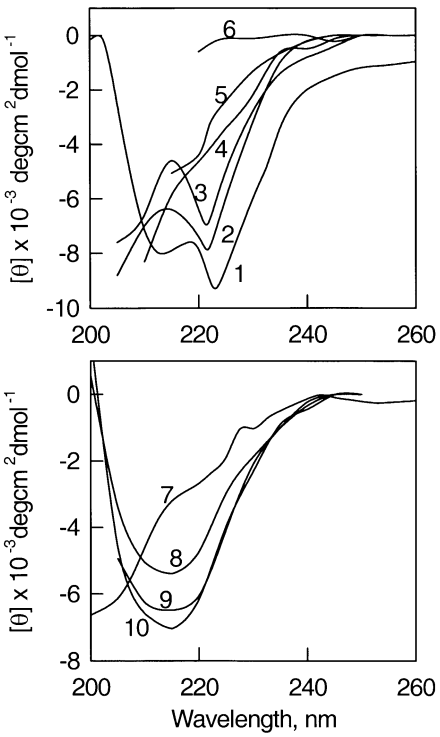

Fig. 8. Far-UV CD spectra of ervatamin B under various conditions. The CD spectra at pH 7.0 (1) and in 6 M GuHCl (6) are shown for comparison. Protein concentration was 0.1 mg/ml. The samples were incubated at the specified conditions for 24 h at 25°C before the measurement. The numbers indicate the far-UV CD spectra of ervatamin B under various conditions (Table 1).

Similarly, the results on the ANS binding to ervatamin B during urea denaturation at pH 3.0 are shown in Fig. 7D. The maximum amount of ANS binding is seen at 0.8 ± 0.1 M urea

Table 1. Structural properties of ervatamin B at different experimental conditions. Ervatamin B is in the native state in 50 mM phosphate buffer, pH 7.0, and the corresponding molar ellipticities in the near and far-UV CD region are considered as 100%. The enzyme was equilibrated under various other conditions, as mentioned in the table below. Their corresponding molar ellipticities were calculated as % structural content for comparison. This represents multiple intermediate states of the enzyme with different structural properties.

Conformational state	Species	Conditions	% ellipticity at 278 nm	% ellipticity at 222 nm
Native	1	pH 7.0	100	100
Intermediate	2	pH 3.0, 0.5 M GuHCl	7	86
Intermediate*	3	pH 3.0, 0.8 M Urea	69	70
Intermediate*	4	pH 4.0, 1.1 M GuHCl	1	51
Intermediate*	5	pH 3.0, 1.95 M Urea	31	36
Denatured	6	6 M GuHCl	0	2
Acid-unfolded	7	pH 2.0, no salt	5	28
Intermediate	8	pH 0.5	0	59
Intermediate	9	pH 2.0, 0.5 M KCl	0	71
Intermediate	10	pH 2.0, 0.25 M GuHCl	0	77

*Intermediates where dominant ANS binding is seen.

concentrations with an increase of eight-fold in fluorescence intensity. Interestingly, another shoulder or inflection on the ANS binding curve with lower fluorescence intensity was observed at 1.9 ± 0.1 M urea.

However, such ANS binding was not observed in urea denaturation at pH 4.0, or at higher pH in the presence of any denaturants. It is to be noted that at pH 3.0, ANS binding was observed at a protein concentration of 0.015 mg/ml, while at pH 4.0 a higher concentration of the protein (0.05 mg/ml) was necessary.

CD spectra of the states with maximum ANS binding In view of the maximum ANS binding that is observed at intermediate concentrations of GuHCl and urea during unfolding, the far-UV CD spectra of ervatamin B at the specific concentrations of the denaturant are shown in Fig. 8. At 0.5 M GuHCl, pH 3.0, the far-UV CD spectrum indicates a high α-helical content, which is close to the helical content of the native enzyme at pH 3.0 (Table 1). However, at 1.1 M GuHCl, pH 4.0, the helical content was much less (Table 1). In 0.8 M urea, pH 3.0, the enzyme showed a helicity of 15%, and the far-UV CD spectrum was predominantly α-helical with the retention of substantial tertiary structure. However, at 1.95 M urea the structural contents were very low (Table 1). Under all of these conditions, the tertiary structure is either drastically reduced or absent with complete loss of proteolytic activity. The far-UV CD spectra of native and denatured ervatamin B are also included in the figure for reference. The far-UV CD spectra of ervatamin B in the intermediate conformations in the acid unfolding pathway, where significant ANS binding was observed, are also shown.

Discussion

The physicochemical characteristics of ervatamin B have been elucidated to get an insight into the structure-function relationship of the enzyme in view of its stability towards pH and denaturants. Circular dichroism, absorbance, and intrinsic fluorescence (along with activity measurements) were used to study the solution conformation of ervatamin B, as well as its unfolding by various denaturants. Ervatamin B belongs to the α + β class of proteins, as seen by CD, and members of this class present separate α-helix and β-sheet rich regions (Levitt and Chothia, 1976). This is actually the case in papain, whose molecule has an all-α domain and an antiparallel β-sheet domain (Kamphuis *et al.*, 1984). Though only preliminary X-ray data for ervatamin B crystals have been obtained in our laboratory (Chakrabarti *et al.*, 1999), and the structure solution is in progress, it may be safely concluded from the CD data that ervatamin B also belongs to the α + β class. The overall CD spectrum of ervatamin B is comparable to papain, chymopapain (Solis-Mendiola *et al.*, 1992), and ervatamin C (Kundu *et al.*, 1999), but it differed from them in some finer details. For example, the negative peak at 295 nm in the near-UV CD spectra of ervatamin B is more intense than in papain. Also, in ervatamin B the negative signal at 222 nm is more intense than the signal at 208 nm, which is unlike ervatamin C, where the reverse is true. Thus, like papain, ervatamin B retained all of the native features in the pH range 3-11, indicating high rigidity of the molecule, but it is less stable than ervatamin C (Kundu *et al.*, 1999).

Acid induced unfolding Acid induced changes of ervatamin B as a function of pH indicate that the protein is structurally and functionally stable over a pH range of 3.0 to 11.0, and loses integrity on either side of this pH range. The acid-induced unfolding transition of ervatamin B in the absence of added salt, was incomplete and appears to involve a conversion from the native state to a somewhat collapsed unfolded state with no tertiary structure and some residual secondary structure along with strong ANS binding (Fig. 3C and 7A). Such a acid-induced state appears to be similar to the acid unfolded states that were observed in cytochrome c and apomyoglobin (Ohgushi and Wada, 1983; Goto and Fink, 1989). At very low pH, the induction of an additional secondary structure was observed, driving the protein into the A-state. In presence of a low-salt concentration, however, the enzyme switches from the native state to the A-state directly. This behavior is typical of the type IC proteins like papain, parvalbumin, and ribonuclease A (Fink *et al.*, 1994). However, compared to other proteins of the type IC, the A-state is observed at very low pH for ervatamin B. Another interesting feature of ervatamin B in the A-state is the change in the nature of the far-UV CD spectrum, which is predominantly of β-sheet, unlike the native state.

Similarly, the dependence of intrinsic fluorescence properties (emission maximum and intensity) of ervatamin B as function of pH also reveals that the enzyme is stable in the pH range of 3.0 to 11.0. Thus, the focus needs to be on the status of the enzyme at very low pH. Any subtle changes in the molecular structure of the enzyme, especially at low pH, should reflect in its stability towards chemical denaturants and temperature, etc. Therefore, urea and GuHCl-induced unfolding of ervatamin B at low pH is carried out. The equilibrium unfolding of ervatamin B by various denaturants also reveal the high stability of the enzyme. The enzyme retains all of its structure and activity over a wide range of pH, and falls only beyond this range. It retains activity in the presence of urea, under neutral conditions, as does papain. However, like papain (Kimmel and Smith, 1957) and unlike ervatamin C (Sundd *et al.*, 1998), it is completely susceptible to urea at low pH. The denaturation characteristics of ervatamin B are different from papain (Hernandez-Arana and Soriano-Carcia, 1988; Xiao *et al.*, 1993; Edwin and Jagannadham, 1998), or ervatamin C (Kundu *et al.*, 1999). Ervatamin B also differs from other proteases in its intrinsic fluorescence and ANS binding properties. These observations, together with the difference in CD spectra, probably suggest a different folding pattern and structural integrity for ervatamin B.

Urea-induced unfolding Under neutral conditions, urea induced no unfolding of ervatamin B, and the protein was active. However, urea-unfolding studies at low pH (3.0 and 4.0) yielded some interesting results. At pH 4.0, the urea-induced unfolding curves that were obtained by various measures were sigmoidal and coincidental (Fig. 6A) showing the absence of intermediates in the unfolding pathway. At pH 3.0, urea induced unfolding of ervatamin B takes place at lower concentrations while the unfolding characteristics are different. All the structural and functional changes occur between 0.25 and 3 M urea and the transition curves are coincidental. Further, the individual transitions obtained by various method are biphasic in nature (Fig. 6B). However, at pH 2.0, low concentration of urea did not induce any structure in the enzyme as in the case of GuHCl.

The most interesting and unique characteristic of ervatamin B is the ANS binding that is observed not only at low pH, but also during chemical induced denaturation. The maximum amount of ANS binding is seen at the 0.8 ± 0.1 M urea concentration, and another shoulder or inflection on the ANS binding curve with lower fluorescence intensity was observed at 1.9 ± 0.1 M urea (Fig. 7D). Moreover, the transition midpoints in urea denaturation (Fig. 6B) coincide with the respective denaturant concentration where ANS binding was dominant. Such intermediates, in the presence of denaturants and the concomitant ANS binding, are a unique property of ervatamin B among the plant cysteine proteases of the papain superfamily. They may have implications in the kinetic pathway of protein folding. However, such ANS binding was not observed in urea denaturation at pH 4.0, or at higher pH in the presence of denaturants.

GuHCl-induced unfolding The GuHCl-induced changes of ervatamin B were followed by various probes (ellipticity at 278 nm and 220 nm), fluorescence (wavelength emission maximum), and activity (Fig. 5). Under neutral conditions, the chemical-induced transition curves were sigmoidal, and all of the structural changes took place between 2.35-4.0 M GuHCl with similar transition mid-points. With the lowering of the pH, the unfolding transition curves are sigmoidal, but become non-coincidental, reflecting the presence of intermediates in the unfolding pathway. Denaturation of ervatamin B starts at a very low concentration of GuHCl at pH 4.0. The overall characteristics of GuHCl-induced unfolding of ervatamin B at pH 3.0 were similar to that observed at pH 4.0, and the activity and other structural parameters were lost in a similar order, but with lower mid-points. Further lowering of pH below 3.0 disrupts all of the tertiary structure with a complete loss of proteolytic activity. The loss in secondary structure followed a single transition with a lower transition midpoint. Thus, GuHCl completely unfolds the partially denatured acid-unfolded state of ervatamin B. Further, it is to be noted that at low concentrations of GuHCl (0.25 M) far-UV CD spectra is predominantly β-sheeted, with a shape similar to the A-state that is seen in acid-induced unfolding. This indicates that GuHCl stabilizes this state, and shows a transition mid-point that is higher than those at pH 3.0 and 4.0. Similarly, the GuHCl-induced unfolding of ervatamin B at a very low pH (0.5) also followed a single transition.

The other interesting and unique characteristic of ervatamin B is the ANS binding that is observed not only at low pH, but also during GuHCl denaturation. The maximum amount of ANS binding that is seen at intermediate concentrations of GuHCl during denaturation (both at pH 3.0 and 4.0) coincides with the transition midpoints (Fig. 7B and 7C).

Conclusions The present investigation identified a number of forms of ervatamin B under various conditions (Table 1). The presence of such multiple equilibrium partially-folded intermediates that differed in the amount of secondary structure, globularity, stability, and compactness have been reported in other proteins (Uversky *et al.*, 1998; Tcherkasskaya and Ptitsyn, 1999; Uversky *et al.*, 1999). They may play an important role in the correct folding of the enzyme. It is being speculated that these partially-folded intermediates probably consist of ensembles of substrates with a common core of native-like secondary structure, which is responsible for their stability. Consequently, it is likely that the intermediates may represent the equilibrium counterparts of transient kinetic intermediates (Uversky *et al.*, 1998).

All of the intermediates had a substantial secondary structure, as well as a strong binding to ANS. In addition, species 2, 4, 8, 9, and 10 have no proteolytic activity or tertiary structure. All of the characteristics of these forms of ervatamin B are typical of molten globule state (Ptitsyn, 1995), and the states seem to be molten globule-like as in some other proteins (Kuwajima *et al.*, 1976; Nozaka *et al.*, 1978; Kim and Baldwin 1982; Goto *et al.*, 1990a, b; Zerovnik *et al.*, 1999).

The equilibrium unfolding of ervatamin B at higher pH (> 4.0) is cooperative, and the protein molecule unfolds as a single entity. The similarity in denaturation curves that were obtained by various measures indicates that the changes in the environment of the excitable tryptophan residues, as well as the changes in secondary and tertiary structure, occur concurrently. Such unfolding transitions can be fitted to two-state mechanism (N→D) under equilibrium conditions, as in the case of small proteins (Privalov, 1979; Kim and Baldwin, 1982). However, the presence of a number of intermediate states in ervatamin B is inconsistent with the simple two-state folding behavior.

In GuHCl denaturation at pH 3.0, an intermediate is observed with a higher secondary structure, but very little tertiary structure along with the strong ANS binding. The GuHCl concentration, where the ANS binding was maximum, was approximately the same as the c_m of the transition curve that was followed by wavelength maxima of intrinsic fluorescence. In GuHCl denaturation at pH 4.0, another intermediate was seen with a lesser secondary structure with no tertiary structure, which appears like the denatured state

with considerable ANS binding. The GuHCl concentrations, where the ANS binding was maximum both at pH 3.0 and 4.0, coincided with the transition midpoint (c_m) of the GuHCl-induced unfolding curve that was obtained by fluorescence emission maximum. On the other hand, two intermediate states are observed during urea induced unfolding ervatamin B at pH 3.0. One intermediate had a high secondary structural content along with a substantial tertiary structure at low urea concentration, while the other had a lower secondary and tertiary structural content at a higher concentration of urea. The binding of ANS was also maximum at two urea concentrations, which coincided roughly with the transition midpoints (c_m) of urea-induced unfolding that was obtained by fluorescence emission maximum. Hence, the equilibrium-unfolding pathway of ervatamin B involves two intermediates, one is native-like while the other resembles the denatured state. It can be generalized as,

$$N \xrightarrow{\text{GuHCL/Urea}} I_1 \xrightarrow{\text{GuHCL/Urea}} I_2 \xrightarrow{\text{GuHCL/Urea}} D$$

However, it should be noted that I_1 and I_2 are not the same states in the urea and GuHCl-induced unfolding pathway. I_1 and I_2 in the urea-induced unfolding with substantial tertiary structure are similar to the intermediate that was reported by Marmorino *et al.* (1998). Therefore, it is likely that the first state with high structural content is probably an early intermediate, while the second one is a late intermediate in the protein unfolding. Similar observations have not been reported in papain or other proteases of the papain superfamily.

This conclusion probably implies that different structural parts of the molecule are stabilized differentially in presence of denaturants, and they unfold sequentially. The different structural parts may be different domains in the enzyme; therefore, they provide evidence for the presence of domains in ervatamin B. In the case of cardiac troponin I (Morjana and Tal, 1998), the urea denaturation curves are biphasic, which indicates the presence of a stable folding intermediate, which might be related to the two-domain architecture of troponin I. Similar observations have suggested the presence of domains in the hormone-sensitive lipase (Osterlund *et al.*, 1999) structure also.

Acknowledgments The financial assistance from the University Grants Commission, Council of Scientific and Industrial Research, and the Department of Biotechnology, India is acknowledged. Authors thank Dr. P K Ambhast for his help in refining the manuscript.

References

Arai, M. and Kuwajima, K. (1996) Rapid formation of a molten globule intermediate in refolding of alpha-lactalbumin. *Folding and Design* **1**, 275-287.

Balasubramanian, D. and Kumar, C. (1976) Recent studies of the circular dichroism and optical rotatory dispersion of biopolymers. *Applied Spectroscopy Reviews* **11**, 223-286.

Bychkova, V. E., Dujsekina, A. E., Klenin, S. I., Tiktopulo, E. I., Uversky, V. N. and Ptitsyn, O. B. (1996) Molten globule-like state of cytochrome c under conditions simulating those near the membrane surface. *Biochemistry* **35**, 6058-6063.

Chakrabarti, C., Biswas, S., Kundu, S., Sundd, M., Jagannadham, M. V. and Dattagupta, J. K. (1999) Crystallization and preliminary X-ray analysis of ervatamin B and C, two thiol proteases from *Ervatamia coronaria*. *Acta Crystallogr.* **D55**, 1074-1075.

Chen, Y. H., Yang, J. T. and Martinez, H. M. (1972) Determination of the secondary structures of proteins by circular dichroism and optical rotatory dispersion. *Biochemistry* **11**, 4120-4131.

Dobson, C. M. (1992) Unfolded proteins, compact states and molten globules. *Curr. Opin. Struct. Biol*. **2**, 6-12.

Edwin, F. and Jagannadham, M. V. (1998) Sequential unfolding of papain in molten globule state. *Biochem. Biophys. Res. Comm*. **252**, 654-660.

Fink, A. L., Calciano, L. J., Goto, Y., Kurotsu, T. and Palleros, D. R. (1994) Classification of acid denaturation of proteins: intermediates and unfolded states. *Biochemistry* **33**, 12504-12511.

Garel, J. R. (1992) Folding of large proteins: Multidomain and multisubunit proteins; in *Protein Folding*, Creighton, T. E. (ed.), pp. 405-454. Freeman, New York, New York.

Gast, K., Zirwer, D., Muller-Frohne, M. and Damaschun, G. (1998) Compactness of the kinetic molten globule of bovine alpha-lactalbumin: a dynamic light scattering study. *Protein Sci.* **7**, 2004-2011.

Goto, Y. and Fink, A. L. (1989) Conformational states of β-lactamase: molten-globule states at acidic and alkaline pH with high salt. *Biochemistry* **28**, 945-952.

Goto, Y., Calciano, L. J. and Fink, A. L. (1990a) Acid-induced folding of proteins. *Proc. Natl. Acad. Sci. USA* **87**, 573-577.

Goto, Y., Takahashi, N. and Fink, A. L. (1990b) Mechanism of acid-induced folding of proteins. *Biochemistry* **29**, 3480-3488.

Harding, M. M., Williams, D. H. and Woolfson, D. N. (1991) Characterization of a partially denatured state of a protein by two-dimensional NMR: reduction of the hydrophobic interactions in ubiquitin. *Biochemistry* **30**, 3120-3128.

Hernandez-Arana, A. and Soriano-Garcia, M. (1988) Detection and characterization by circular dichroism of a stable intermediate state formed in the thermal unfolding of papain. *Biochim. Biophys. Acta* **954**, 170-175.

Kamphuis, I. G., Kalk, K. H., Swarte, M. B. and Drenth, J. (1984) Structure of papain refined at 1.65Å resolution. *J. Mol. Biol*. **179**, 233-256.

Khorasanizadeh, S., Peters, I. D., Butt, T. R. and Roder. H. (1993) Folding and stability of a tryptophan containing mutant of ubiquitin. *Biochemistry* **32**, 7054-7063.

Khurana, R., and Udgaonkar, J. B. (1994) Equilibrium unfolding studies of barstar: evidence for an alternative conformation which resembles a molten globule. *Biochemistry* **33**, 106-115.

Kim, P. S. and Baldwin R. L. (1982) Specific intermediates in the folding reactions of small proteins and the mechanism of protein folding. *Annu. Rev. Biochem*. **51**, 459-489.

Kim, P. S. and Baldwin, R. L. (1990) Intermediates in the folding reactions of small proteins. *Annu. Rev. Biochem*. **59**, 631-660.

Kimmel, J. R. and Smith, E. L. (1957) The properties of papain.

Adv. Enzymol. **19**, 267-334.

Kundu, S., Sundd, M. and Jagannadham, M. V. (1999) Structural characterization of a highly stable cysteine protease ervatamin C. *Biochem. Biophys. Res. Commun*. **264**, 635-642.

Kundu, S., Sundd, M. and Jagannadham, M. V. (2000) Purification and characterization of a stable cysteine protease ervatamin B, with two disulfide bridges, from the latex of *Ervatamia coronaria*. *J. Agric. Food Chem*. **48**, 171-179.

Kuwajima, K., Nitta, K., Yoneyama, M. and Sugai, S. (1976) Three state denaturation of α-lactalbumin by guanidine hydrochloride. *J. Mol. Biol*. **106**, 359-373.

Kuwajima, K., Semisotnov, G. V., Finkelstein, A. V., Sugai, S. and Ptitsyn, O. B. (1993) Secondary structure of globular proteins at the early and the final stages in protein folding. *FEBS Lett*. **334**, 265-268.

Levitt, M., and Chothia, C. (1976) Structural patterns in globular proteins. *Nature* **261**, 552-558.

Manavalan, P. and Johnson, W. C. (1983) Sensitivity of circular dichroism to protein tertiary structure class. *Nature* **305**, 831-832.

Marmorino, J. L., Lehti, M. and Pielak, G. J. (1998) Native tertiary structure in an A-state. *J. Mol. Biol* **275**, 379-388.

Morjana, N. and Tal., R. (1998) Expression and equilibrium denaturation of cardiac troponin I: stabilization of a folding intermediate during denaturation by urea. *Biotechnol. Appl. Biochem.* **28**, 7-17.

Nozaka, M., Kuwajima, K., Nitta, K. and Sugai, S. (1978) Detection and characterization of the intermediate on the folding pathway of human α-lactalbumin. *Biochemistry* **17**, 3753-3758.

Ohgushi, M. and Wada, A. (1983) Molten-globule state: a compact form of globular proteins with mobile side chains. *FEBS Lett.* **164**, 21-24.

Osterlund, T., Beussman, D. J., Julenius, K., Poon, P. H., Linse, S., Shabanowitz, J., Hunt, D. F., Schotz, M. C., Derewenda, Z. S. and Holm, C. (1999) Domain identification of hormone-sensitive lipase by circular dichroism and fluorescence spectroscopy, limited proteolysis and mass spectrometry. *J. Biol. Chem*. **274**, 15382-15388.

Privalov, P. L. (1979) Stability of proteins: small globular proteins. *Adv. Protein Chem*. **33**, 167- 241.

Ptitsyn, O. B. (1992) The molten globule state; in *Protein Folding*, Creighton, T. E. (ed.), pp. 243-300. Freeman, New York, New York.

Ptitsyn, O. B. (1995) Molten globule and protein folding. *Adv. Protein Chem*. **47**, 83-229.

Ptitsyn, O. B., Pain, R. H., Semisotnov, G. V., Zerovnik, E. and Razgulyaev, O. I. (1990) Evidence for a molten globule state as a general intermediate in protein folding. *FEBS Lett.* **262**, 20-24.

Schmid, F. X. (1989) Spectral methods of characterizing protein conformation and conformational changes. In *Protein Structure: A Practical Approach*, (Creighton, T.E., ed.), pp. 251-285. IRL Press, Oxford, U.K.

Semisotnov, G. V., Rodionova, N. A., Razgulyaev, O. I., Uversky, V. N., Gripas, A. F. and Gilmanshin, R. I. (1991) Study of the molten globule intermediate state in protein folding by a hydrophobic fluorescent probe. *Biopolymers* **31**, 119-128.

Shirley, B. A. (1995) Urea and guanidine hydrochloride denaturation curves. In *Protein Folding and Stability*, Shirley, B. A. (Eds) pp. 177-190, Humana Press, Totowa, New Jersey.

Solis-Mendiola, S., Arroyo-Reyna, A. and Hernandez-Arana, A. (1992) Circular dichroism of cysteine proteinases from papaya latex. Evidence of differences in the folding of their polypeptide chains. *Biochim. Biophys. Acta* **1118**, 288-292.

Strickland, E. H. (1974) Aromatic contributions to circular dichroism spectra of proteins. *CRC Crit. Rev. Biochem*. **2**, 113-175.

Strickland, E. H., Hortwiz, J. and Billups, C. (1969) Fine structure in the near-ultraviolet circular dichroism and absorption spectra of tryptophan derivatives and chymotrypsinogen A at 77°K. *Biochemistry* **8**, 3205-3213.

Sundd, M., Kundu, S., Pal, G. P. and Medicherla, J. V. (1998) Purification and characterization of a highly stable cysteine protease from the latex of *Ervatamia coronaria*. *Biosci. Biotech. Biochem*. **62**, 1947-1955.

Tcherkasskaya, O. and Ptitsyn, O. B. (1999) Molten globule versus variety of intermediates: influence of anions on pH-denatured apomyoglobin. *FEBS Lett*. **455**, 325-331.

Uversky, V. N., Karnoup, A. S., Khurana, R., Segel, D. J., Doniach, S. and Fink, A. L. (1999) Association of partially folded intermediates of Staphylococcal nuclease induces structure and stability. *Protein Sci.* **8**, 161-173.

Uversky, V. N., Karnoup, A. S., Segel, D. J., Seshadri, S., Doniach, S. and Fink, A. L. (1998) Anion-induced folding of Staphylococcal nuclease: characterization of multiple equilibrium partially folded intermediates. *J. Mol. Biol*. **278**, 879-894.

Xiao, J., Liang, S. -J. and Tsou, C. -L. (1993) Inactivation before significant conformational change during denaturation of papain by guanidine hydrochloride. *Biochim. Biophys. Acta* **1164**, 54-60.

Zerovnik, E., Janjic, V., Francky, A. and Mozetic-Francky, B. (1999) Equilibrium and transient intermediates in folding of human macrophage migration inhibitory factor. *Eur. J. Biochem*. **260**, 609-618.